EMERGENCE OF ORGANIZED BURSTING IN CLUSTERS OF PANCREATIC β-CELLS BY CHANNEL SHARING

ARTHUR SHERMAN,* JOHN RINZEL,* AND JOEL KEIZER‡
*National Institutes of Health, National Institute of Diabetes and Digestive and Kidney Diseases-Mathematical Research Branch, Bethesda, Maryland 20892; and ‡Institute of Theoretical Dynamics and Department of Chemistry, University of California-Davis, Davis, California 95616

ABSTRACT Pancreatic β-cells in an intact Islet of Langerhans exhibit bursting electrical behavior. The Chay-Keizer model describes this using a calcium-activated potassium (K-Ca) channel, but cannot account for the irregular spiking of isolated β-cells. Atwater I., L. Rosario, and E. Rojas, *Cell Calcium.* 4:451–461, proposed that the K-Ca channels, which are rarely open, are shared by several cells. This suggests that the chaotic behavior of isolated cells is stochastic. We have revised the Chay-Keizer model to incorporate voltage clamp data of Rorsman and Trube and extended it to include stochastic K-Ca channels. This model can describe the behavior of single cells, as well as that of clusters of cells tightly coupled by gap junctions. As the size of the clusters is increased, the electrical activity shows a transition from chaotic spiking to regular bursting. Although the model of coupling is over-simplified, the simulations lend support to the hypothesis that bursting is the result of channel sharing.

I. INTRODUCTION

The Islets of Langerhans in the pancreas secrete insulin in response to the level of glucose in the blood, thereby maintaining the glucose level within a narrow operating range. There are several million such islets, and each contains several thousand insulin secreting cells, known as β-cells, as well as other types of cells. The release of insulin is pulsatile and is correllated with rhythmic oscillations in membrane potential. If one impales a β-cell in an isolated islet exposed to glucose with a microelectrode, one observes a slow oscillation from a low voltage (silent phase) to a plateau upon which is superimposed rapid spiking (active phase). This phenomenon is commonly called bursting. See Fig. 1 *a*.

Calcium flows into the cell during spiking (Dean and Mathews, 1970; Rorsman and Trube, 1986), and this increase in intracellular calcium is believed to cause insulin release (Rubin, 1982). The fraction of time spent spiking increases with extra-cellular glucose concentration (Beigelman et al., 1977). In order to explain the electrical aspects of this behavior Atwater et al. (1980) proposed a mechanism based on voltage-gated potassium and calcium channels and a calcium-activated potassium (K-Ca) channel. Chay and Keizer (1983) developed these ideas into a quantitative, dynamic model, which accounted well for a number of observations made in the islet preparation. In the absence of voltage clamp data for the β-cell, this model was based on modifications of Hodgkin-Huxley kinetics for the squid giant axon.

Within an islet, β-cells are known to be electrically coupled and bursting is approximately synchronous. The Chay-Keizer model describes the electrical behavior only of a representative cell in an intact, perfectly synchronized, islet. On the other hand, β-cells burst only when coupled in the islet (or artificially clumped together in vitro). Single cells exhibit irregular spiking, as shown in Fig. 1 *c*, from Rorsman and Trube (1986). We cannot conceive of any modification of the Chay-Keizer model involving only coupling and deterministic mechanisms that can account for both the single-cell and cell cluster behavior. Thus, in pursuing our long-term goal of understanding bursting and synchronized activity in the β-cell, we have been led to consider stochastic mechanisms.

We focus on a stochastic explanation of the effects of coupling called channel sharing, first advanced by Atwater et al. (1983). These authors noted that the conductance of a single K-Ca channel is large compared with the total K^+ conductance of the β-cell and that the K-Ca channels are open very rarely under physiological voltages and intracellular calcium concentrations (Findlay et al., 1985). They inferred that the resting potential would be unstable unless the cells shared channels by electrical coupling through gap junctions. If very few of these channels are open at any given time, then random channel events may perturb the membrane potential of an isolated cell enough to disrupt the burst pattern and produce the observed irregular behavior of single cells. In clusters (islets or clumps) of electrically-coupled β-cells, on the other hand, regular bursting might be possible because the contribution of each

Address correspondence to Dr. Arthur Sherman, National Institutes of Health, National Institute of Diabetes and Digestive and Kidney Diseases-Mathematical Research Branch, Building 31, Room 4B-54, Bethesda, MD 20892.

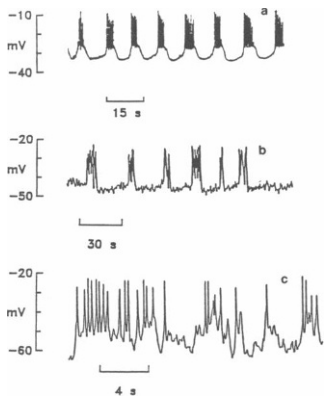

FIGURE 1 (*a*) Recording from a representative β-cell in an intact islet in 11 mM glucose. Taken from Atwater and Rinzel, 1986. (*b*) Recording from a 70-μm diameter cluster of cultured β-cells exposed to 10 mM glucose. Reprinted with permission from Rorsman and Trube, 1986, Fig. 1 *a*. (*c*) Spontaneous spiking from an isolated β-cell exposed to 10 mM glucose. Reprinted with permission from Rorsman and Trube, 1986, Fig. 2 *c*.

channel to the current density in the shared membrane, and hence the perturbing effect of each channel event, would be smaller. By incorporating a stochastic K-Ca channel into a revised version of the Chay-Keizer model we demonstrate here the viability of the channel-sharing hypothesis. Bangham et al. (1986) presented a single-cell model that had stochastic K^+ channels and exhibited irregular spiking. They did not, however, model cell clusters and so did not address the channel-sharing hypothesis or consider the emergence of bursting in large clusters of cells.

It is tempting to dismiss the importance of K-Ca channels for bursting because they are open so rarely. Thus, a number of alternative molecular mechanisms for bursting, all involving slow feedback of calcium onto inward or outward currents, have been proposed and explored theoretically. For a review see (Keizer, 1988). Our simulations suggest, however, not only that the K-Ca channels may play a role in bursting, but that they must necessarily be open a small fraction of the time for organized bursting to occur. Our general conclusions about channel sharing in cell clusters are independent of the precise mechanism of calcium feedback. In fact, Chay and Kang (1988) have obtained similar results using a model based on calcium inactivation of a calcium channel and different simulation techniques.

In order to base our investigation more solidly in experimental facts, we have updated the Chay-Keizer model by incorporating recent experiments of Rorsman and Trube (1986) that characterize the voltage-gated potassium and calcium currents in the β-cell. The details of this are given in Section II, where we formulate a deterministic model for a representative β-cell in a synchronized islet. Section III introduces a model for an isolated β-cell with a finite number of stochastic K-Ca channels. In Section IV this treatment is extended to a cluster of tightly-coupled stochastic β-cells. We demonstrate that, as the number of cells in the cluster is increased, there is a transition from irregular spiking to bursting. We also draw some theoretical conclusions from our simulations about channel sharing. We show how the results depend on the unitary conductance and density of the shared channel. This is important because these parameters are not precisely known at the present time. In Section V we critique the model and discuss its applicability to the β-cell. We conclude with suggested issues for experimenters to investigate in light of the model's predictions.[1]

II. DETERMINISTIC MODEL FOR A REPRESENTATIVE CELL IN A SYNCHRONIZED ISLET

Voltage-Dependent Currents and Action Potential Generation

We base our model for the representative β-cell on whole-cell voltage clamp experiments performed at 20–22 °C by Rorsman and Trube (1986). After the usual Hodgkin-Huxley formulation, individual ionic currents are represented as products of voltage and time-dependent conductances with driving potentials that reverse at the Nernst equilibrium potential. Each conductance is expressed as the product of the total cell conductance and the activation level, or fraction of channels open. With modifications, as described below, we use the measured values for parameters and theoretical expressions for activation levels given by Rorsman and Trube. The exact parameter values and equations are given in the Appendix. The most salient experimental facts are (*a*) There is a voltage-gated Ca^{2+} conductance whose steady-state activation curve is given by the sigmoidal function

$$m_\infty(V)^\rho = \frac{1}{1 + \exp[(V_m - V)/S_m]}, \qquad (2.1)$$

with $V_m = 4.0$ mV and $S_m = 14.0$ mV. (*b*) There is a voltage-gated K^+ conductance with sigmoidal activation curve

$$n_\infty(V)^\mu = \frac{1}{1 + \exp[(V_n - V)/S_n]}, \qquad (2.2)$$

with $V_n = -19.0$ mV and $S_n = 5.6$ mV. (*c*) No data are given to choose values for the exponents ρ and μ, or for the presence of a leakage current. (*d*) From whole-cell current measurements and the above activation curves we estimate that the maximal Ca^{2+} and K^+ conductances, $\bar{g}_{Ca}$ and $\bar{g}_K$,

[1]Preliminary reports on this work have appeared in an abstract (Sherman, A., J. Rinzel, and J. Keizer, 1988. *Biophys. J.* Vol. 53:518*a* [Abstr.]) and a conference proceedings (Rinzel, J. 1988. On the electrical activity and glucose response of insulin-secreting cells. *In* Biomathematics and Related Computational Problems. L. Ricciardi, editor. 685–696. D. Reidel Publishing Co., Dordrecht, Holland.)

are on the order of several thousand pS, with $\bar{g}_K$ about twice as big as $\bar{g}_{Ca}$. (*e*) In the range of voltages of interest for bursting, the time constants for the Ca^{2+} and K^+ currents, respectively $\tau_m(V)$ and $\tau_n(V)$, are $\tau_m \approx 0.15$–1.5 ms and $\tau_n \approx 20$–30 ms.

Because the time constant for the Ca^{2+} current is so small, we chose to set $m(t) = m_\infty(V)$; in this case the value of ρ does not matter, so we let $\rho = 1$. For μ we used the value 1 (although variations of the model with $\mu = 2$ and a correspondingly modified n_∞ also gave reasonable results). We found that by adjusting V_n slightly, to -15 mV, the model became much more robust under perturbations and changes in other parameters. A formula for $\tau_n(V)$ was obtained by fitting a function of the form

$$\tau_n(V) = \frac{c}{\exp[(V - \bar{V})/a] + \exp(-(V - \bar{V})/b)} \quad (2.3)$$

to the given experimental values. The leakage current was found to be inessential.

We found that the standard current-voltage (*I-V*) relation, based on Ohm's law and the Nernst equation, is inadequate to describe all of Rorsman and Trube's (Rorsman and Trube, 1986) data for the Ca^{2+} current. We obtained an improved fit to the experimental *I-V* curve by multiplying the current by a reverse sigmoidal factor,

$$h(V) = \frac{1}{1 + \exp[(V - V_h)/S_h]}, \quad (2.4)$$

with $V_h = -10$ mV and $S_h = 10$ mV. The product of $h(V)(V - V_{Ca})$ with the single-channel conductance can be interpreted as a nonlinear *I-V* relation for a single open calcium channel. Although we can offer no channel model which results in this *I-V* relation, it does give a reasonable fit to the experimental *I-V* curves (Fig. 2) in Rorsman and Trube. The shape is much closer to the experimental curves than that of a linear *I-V* relation, and the scale is within a factor of ⅓. In particular, for the case $[Ca]_o = 2.56$ mM, it reproduces the early peak and sharp dropoff in the calcium current. This representation does not, however, adequately

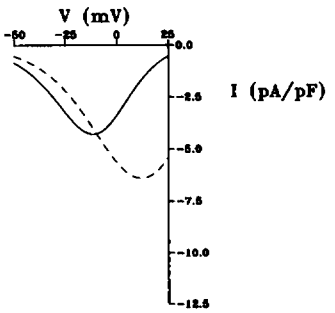

FIGURE 2 (*Solid curve*) $I_{Ca}(V) = g_{Ca}m_\infty(V)h(V)(V - 110)$. (*Dashed curve*) $I_{Ca}(V) = g_{Ca}m_\infty(V)(V - 50)$. Including factor $h(V)$ gives much better agreement with the shape of the experimental calcium *I-V* curve (See Rorsman and Trube, 1986, Fig. 3 *a*).

model the shift in the *I-V* curve as $[Ca]_o$ is varied. Other investigators have used the Goldman-Hodgkin-Katz equation (Hodgkin and Katz, 1949; Goldman, 1943) to model calcium channels in other preparations. See, for example, Kay and Wong (1986) on the guinea-pig hippocampal neuron and Morris and Lecar (1981) for the case of barnacle muscle fibers. We found that this approach did not adequately capture the early peak in I_{Ca}, nor were we able to generate solutions with correctly shaped bursts using that formulation.

The equations which describe the action-potential dynamics of our model are given by:

$$C_m \frac{dV}{dt} = -I_K - I_{Ca} - I_{K\text{-}Ca} = -\bar{g}_K n(V - V_K) - \bar{g}_{Ca} m_\infty(V)h(V)(V - V_{Ca}) - g_{K\text{-}Ca}(V - V_K) \quad (2.5)$$

$$\frac{dn}{dt} = \lambda\left[\frac{n_\infty(V) - n}{\tau_n(V)}\right], \quad (2.6)$$

where C_m is the total membrane capacitance of the cell; V_K and V_{Ca} are the K^+ and Ca^{2+} reversal potentials, respectively; and λ is a nondimensional parameter, analogous to the temperature in the Hodgkin-Huxley model, which we have used to fine tune the K^+ time constant. Here we have included the calcium-activated potassium current, $I_{K\text{-}Ca}$, but, for now, we treat the conductance $g_{K\text{-}Ca}$ as a parameter. If λ is near 1, the system exhibits action-potential oscillations over a large, but bounded interval of $g_{K\text{-}Ca}$ values.

Our calculations confirm the suggestion of Rorsman and Trube (Rorsman and Trube, 1986, p. 532) that the voltage-gated calcium and potassium currents described above are sufficient to generate the action potentials of the β-cell. Chay (1987) also obtains action potentials with a two-current model of the β-cell that is based in part on the Rorsman and Trube data. In order to obtain bursting she employs calcium inactivation of the calcium conductance as a feedback mechanism, rather than a calcium-activated potassium conductance. While the activation parameters and time constants for our voltage-gated potassium and calcium currents are more faithful to those given by Rorsman and Trube, we have not incorporated all of their observations. In particular, we have neglected the slow voltage-dependent inactivation of I_K. With only minor adjustment of other parameters this inactivation can be incorporated in our model, but it does not change the results qualitatively, so we have not included it in the calculations below.

Bursting by Calcium Feedback

In order to formulate a bursting mechanism and analyze it, we follow the ideas of Rinzel (1985) on the qualitative structure of the Chay-Keizer model. This treatment exploits the time-scale differences in the fast and slow processes, (i.e., spike generation and calcium feedback to

the K-Ca current, respectively) to show how the cell alternates between the active and silent phases. Since $g_{K\text{-}Ca}$ varies slowly during a burst period, it is helpful to examine how solutions of Eqs. 2.5 and 2.6 depend on $g_{K\text{-}Ca}$ when it is treated as a parameter. First, we define the steady-state current as:

$$I_{SS}(V; g_{K\text{-}Ca}) = \bar{g}_K n_\infty(V)(V - V_K) + \bar{g}_{Ca} m_\infty(V) h(V)(V - V_{Ca}) + g_{K\text{-}Ca}(V - V_K). \quad (2.7)$$

The voltages corresponding to zero crossings of this current represent steady states of the membrane, i.e., time-independent solutions of Eqs. 2.5–2.6. Note that the expression for I_{SS} incorporates the steady-state dependence of n upon V. Fig. 3 *a* is a plot of I_{SS} for several values of $g_{K\text{-}Ca}$. For $g_{K\text{-}Ca}$ large, the single steady-state V is near V_K; for $g_{K\text{-}Ca}$ small, V lies intermediate between V_K and V_{Ca}. There is an intermediate range of $g_{K\text{-}Ca}$ values for which I_{SS} generates three steady states. A concise graphical summary (called a Z-curve) of the steady-state voltages as functions of $g_{K\text{-}Ca}$ is shown in Fig. 3 *b*.

The mathematical stability and, hence, physical realizability of each steady state depends on the values of the parameters in Eqs. 2.5–2.6 (For background on stability analysis see Fitzhugh, 1961). Figs. 3 *b* and 4 *a* illustrate the stability of these steady states with $g_{K\text{-}Ca}$ as a parameter for different values of λ. The equations are called bistable because a low-V stable steady state coexists with a high-V stable steady state or oscillatory state. The intermediate steady state is unstable (*dashed*), and it represents a threshold voltage of saddle type.

If λ is large enough the delayed-rectifier current responds so rapidly to changes in V that the inward and outward currents balance, and there are no oscillations. Thus, for λ = 7 (Fig. 3 *b*) both the high-V and low-V states are stable (*solid*).

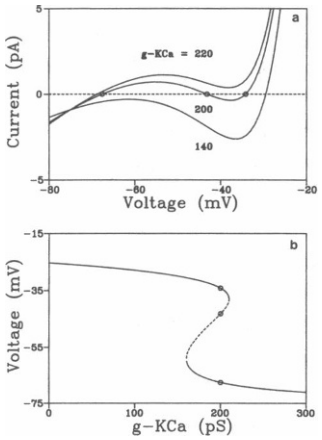

FIGURE 3 (*a*) Steady-state I-V relation for the deterministic model for various values of $g_{K\text{-}Ca}$, Eq. 2.7. (*b*) Z-curve obtained by plotting the zero crossings of $I_{SS}(V; g_{K\text{-}Ca})$ as a function of $g_{K\text{-}Ca}$. Solid portions of curve represent steady states which are stable solutions to Eq. 2.5–2.6, while dashed portions are unstable. Here λ = 7. Stability was computed using the program AUTO (Doedel, 1981). The small circles are the roots of I_{SS} $(V; g_{K\text{-}Ca})$ for $g_{K\text{-}Ca}$ = 200 pS and correspond to the small circles in Fig. 3 *a*.

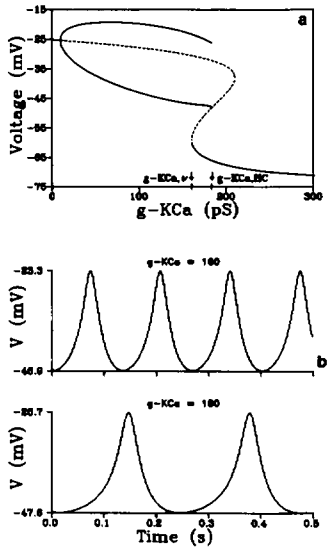

FIGURE 4 (*a*) Bifurcation diagram computed using program AUTO (Doedel, 1981). The Z-curve represents steady states of Eqs. 2.5–2.6. Solid indicates stable, dashed unstable. Here, for λ = 1.6, the high-V steady state is unstable for a range of $g_{K\text{-}Ca}$ values and may be surrounded by an oscillation; the fork on the Z-curve indicates the maximum and minimum voltage of this periodic, repetitive firing, solution as functions of $g_{K\text{-}Ca}$. The left knee of the Z-curve at $g_{K\text{-}Ca,F}$ (= 160.30 pS) is where the low voltage steady-state branch joins the threshold saddle branch. The stable periodic solution branch terminates at $g_{K\text{-}Ca,HC}$ (= 183.26 pS) where the oscillating voltage collides with the saddle branch. As $g_{K\text{-}Ca}$ approaches $g_{K\text{-}Ca,HC}$ the period becomes infinite; the collision point is called a homoclinic point. (*b*) Solution of Eqs. 2.5–2.6 with $g_{K\text{-}Ca}$ = 160 pS (*upper*) and 180 pS (*lower*), corresponding roughly to the spikes seen at the beginning and the end of a burst (see Fig. 5 *a*). Note that the amplitudes change slightly and period almost doubles from the upper panel to the lower.

For λ near 1.6 (Fig. 4 *a*), however, the high-V state may no longer be stable but instead may be surrounded by a periodic oscillation. Such fast time scale oscillations correspond to the repetitive spiking of the active phase. Thus, reading from left to right, at a certain value of $\bar{g}_{K\text{-}Ca}$ (where the fork begins) the upper steady state loses stability and gives rise to a small amplitude oscillation. This event is called a Hopf bifurcation. The upper and lower branches of the fork represent the minimum and maximum voltages attained by the oscillation for the corresponding value of $g_{K\text{-}Ca}$; examples for two selected values of $g_{K\text{-}Ca}$ are shown in Fig. 4 *b*. The time courses were computed by integrating Eqs. 2.5–2.6 with $g_{K\text{-}Ca}$ as a parameter using a Gear algorithm (Gear, 1967). The stability characteristics were computed by the program AUTO (Doedel, 1981). The computations were carried out on a VAX 8600 computer (Digital Equipment Corp., Maynard, MA).

The periodic solutions terminate when the oscillation's minimum voltage just falls below the threshold, i.e., when

the fork's lower branch contacts the intermediate steady state. As $g_{K\text{-}Ca}$ approaches a critical value the period of the oscillatory response tends to infinity; the limiting solution, as it disappears, is called a homoclinic orbit, and we denote the critical value $g_{K\text{-}Ca,HC}$. The left knee of the Z-curve at $g_{K\text{-}Ca,\nu}$ marks the transition from the saddle branch to the low-V steady state.

Bistability is the underlying mechanism for bursting in all existing models of the β-cell. In our model, slow upward and downward variation of $g_{K\text{-}Ca}$ through the range ($g_{K\text{-}Ca,\nu}$, $g_{K\text{-}Ca,HC}$) sweeps the system alternately through active and silent phases. It is necessary that the variations of $g_{K\text{-}Ca}$ be very slow relative to the changes in V and n so that Eqs. 2.5–2.6 are in a quasi-steady state.

The two voltage-gated currents, I_K and I_{Ca}, are delicately balanced, and a small additional current, e.g., $I_{K\text{-}Ca}$, on the order of several pA, can switch the equations between the two regimes. We will see later that the behavior of the stochastic version of the model depends critically on the size of the conductance window Δg ($= g_{K\text{-}Ca,HC} - g_{K\text{-}Ca,\nu}$) which is traversed during an active or silent phase. The size of the window depends sensitively on λ and other parameters.

We have considerable freedom in specifying the characteristics of the slowly varying potassium conductance, $g_{K\text{-}Ca}$, such that it can regulate the bursting. For simplicity, we use the formulation originated by Plant (1978) and adopted by Chay and Keizer (1983). Their idea can be interpreted in terms of a K^+ channel with two possible states, open (O) and closed (C). When a Ca^{2+} ion binds to a closed channel it opens according to the kinetic equations:

$$C + \mathrm{Ca} \underset{k_-}{\overset{k_+}{\rightleftharpoons}} O. \tag{2.8}$$

At equilibrium the relative populations of open and closed states satisfy

$$\frac{[O]}{[C]} = \frac{\mathrm{Ca}_i}{K_d}, \tag{2.8a}$$

where $K_d = k_-/k_+$ and Ca_i is the concentration of free intracellular calcium. Therefore, if the kinetics of the binding process are rapid, we deduce from Eq. 2.8a that the fraction of open channels is $\mathrm{Ca}_i/(K_d + \mathrm{Ca}_i)$ so that

$$g_{K\text{-}Ca}(\mathrm{Ca}_i) = \bar{g}_{K\text{-}Ca} \frac{\mathrm{Ca}_i}{K_d + \mathrm{Ca}_i}. \tag{2.9}$$

The value of Ca_i changes as a result of the inward Ca^{2+} current and because of calcium removal through mitochondrial uptake, pumping, or other unspecified mechanisms. Intracellular calcium (Ca_i) varies slowly because the fraction of free calcium in the cell, f, is taken to be very small ($10^{-3} - 10^{-4}$); this follows from the fact that the bulk of incoming Ca^{2+} is rapidly taken up by high affinity binding sites. Thus, Ca_i satisfies the equation (Chay and Keizer, 1983)

$$\frac{d\mathrm{Ca}_i}{dt} = f(-\alpha I_{Ca} - k_{Ca}\,\mathrm{Ca}_i), \tag{2.10}$$

where α is a unit conversion factor to change current into concentration/time and k_{Ca} is the net Ca^{2+} removal rate. Note that although the fraction of open channels equilibrates instantaneously to the level of intracellular calcium, it varies slowly because it depends only on calcium. Note, also, that the model places no restriction on the value of $\bar{g}_{K\text{-}Ca}$; for appropriate values of f and k_{Ca} the value of Ca_i automatically adjusts to put $g_{K\text{-}Ca}$ in the range for bursting, 150–200 pS (cf, Fig. 4 *a*).

Eqs. 2.5, 2.6, 2.9, and 2.10 constitute the deterministic bursting model. (A full statement of the equations and the parameters is contained in the Appendix.) It would appear to be one of the simplest models consistent with the

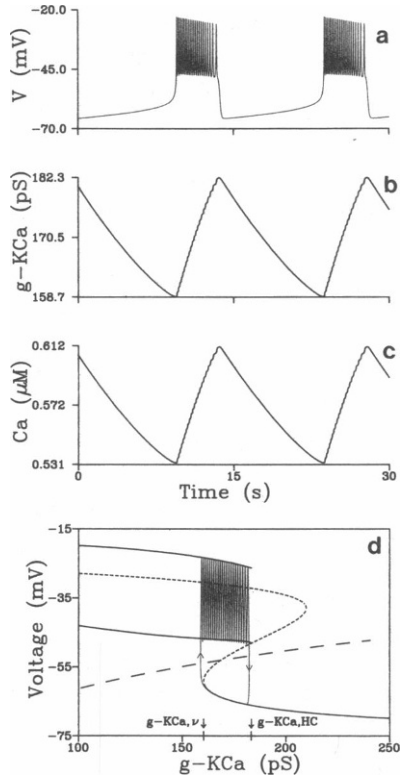

FIGURE 5 Bursting solution for the deterministic model: Voltage, (*a*) calcium-activated potassium conductance, (*b*) and intracellular calcium (*c*) plotted against time. Solutions were obtained by integrating numerically Eqs. 2.5, 2.6, 2.9, and 2.10 using parameter values in the Appendix. The period of the spikes increases from the beginning to the end of a burst. Note that $g_{K\text{-}Ca}$ is essentially a constant multiple of Ca_i because K_d is large. See Eq. 2.9. (*d*) Bursting solution projected as V-$g_{K\text{-}Ca}$ trajectory and overlayed on expanded bifurcation diagram from Fig. 4 *a*. The arrows indicate the direction of increasing time. If V-Ca_i phase plane had been drawn instead, the results would have been indistinguishable except for a scale factor.

Rorsman and Trube data that exhibits bursting. More elaborate internal calcium handling could be substituted for Eq. 2.10 without interfering with the rest of the model. We have ignored the known voltage dependence of the K-Ca channel (Findlay et al., 1985) because present data are not sufficiently accurate in the physiological range of low V and low calcium. As more accurate data become available, channel dynamics with voltage dependence and more complicated calcium dependence could be employed. Other slow potassium channels such as the voltage-independent, ATP-inhibited potassium channel can be added or substituted. Indeed, a model for bursting has been developed which uses the Rorsman and Trube kinetics for K^+ and Ca^{2+} conductances and which incorporates a slowly varying ATP/ADP ratio to modulate the burst (Magnus, 1988).

Figs. 5*a–c* show the voltage, calcium-activated potassium conductance, and calcium time courses obtained by numerical integration of Eqs. 2.5, 2.6, 2.9, and 2.10, while Fig. 5 *d* shows the V-$g_{K\text{-}Ca}$ phase plane trajectory superimposed on an expanded view of the bifurcation diagram, Fig. 4 *a*. These pictures expose the Ca_i feedback mechanism which regulates the burst. During the silent phase Ca_i decreases due to calcium removal (the k_{Ca} term), which turns off the K-Ca channels and slowly depolarizes the cell. When the membrane potential rises above a threshold the voltage dependent K^+ and Ca^{2+} channels open and cause repetitive spiking. The Ca^{2+} channels allow influx of calcium (the I_{Ca} term) into the cell which slowly reactivates the K-Ca channels again, terminating the burst and repolarizing the cell.

Note that $g_{K\text{-}Ca}$ slavishly follows Ca_i; this relationship will be broken in the stochastic model. If we had drawn Figs. 3 *b*, 4 *a*, and 5 *d* in terms of calcium instead of conductance the results would have been indistinguishable except for scale because the calcium dissociation constant K_d is large, and hence $g_{K\text{-}Ca}$ is approximately a constant multiple of Ca_i.

The results depend sensitively on the value of λ, which controls the excitability of the spike generating system and hence the shape of the fork in Figs. 4 *a* and 5 *d*. The computations displayed in Fig. 5 were carried out with $\lambda = 1.6$. Reasonable looking bursts can be obtained for λ in the range (1.5–1.7). As λ is increased the fork closes up on the upper branch so that part of the upper branch of the Z-curve is stable. For λ bigger still the entire upper branch of the Z-curve becomes stable, and bursting is replaced by a slow wave oscillation in which V alternates between the upper and lower steady state branches. This corresponds to the situation in Fig. 3 *b*. On the other hand, if λ is too small the fork opens out below the left knee and $g_{K\text{-}Ca,HC}$ moves leftward to equal $g_{K\text{-}Ca,P}$. In this case bistability is lost, and instead of bursting we find a large amplitude continuous spiking mode called beating.

The structure of the $g_{K\text{-}Ca} - V$ phase plane and the overall behavior of our revised model is qualitatively the same as the Chay-Keizer model, as updated in (Chay and Keizer, 1985); the differences are quantitative. As with their original model, one can simulate the glucose dose response behavior by varying the rate (k_{Ca}) of calcium removal from the cytoplasm. The effects of quinine and tetraethylammonium ion (TEA) can be modeled in the same manner as in the old model (Chay and Keizer, 1983). The spike height, rest potential, and the plateau potential can be adjusted by manipulating λ and V_K. The burst frequency depends almost linearly on f, provided f is sufficiently small. The spike frequency with $\lambda = 1.65$ decreases from ~8 to 4 per s from the beginning to near the end of a burst (comparable to experimental results), with a precipitous drop to near zero frequency just as the burst ends (compare with Fig. 4 *b*). The peak Ca^{2+} and K^+ currents are ~ -20 and 12 pA, respectively, during the active phase, about twice the Chay-Keizer values. The net current varies between ± 5–10 pA during the active phase. The only area of major discrepancy between the two models is the predicted range of values of $g_{K\text{-}Ca}$. The new model gives a range of 150–200 pS, which is ten times greater than in the Chay-Keizer model and about two or three times the value estimated from rubidium flux experiments (Atwater et al., 1983).

This completes our discussion of the revised deterministic model. It provides an adequate quantitative description of the behavior of a typical β-cell in a synchronized islet. As indicated at the beginning, however, it does not predict the irregular behavior of isolated cells. In order to achieve this we turn to a stochastic description.

III. STOCHASTIC MODEL FOR AN ISOLATED β-CELL

Patch clamp experiments on the K-Ca channel show that it has a large unitary conductance of ~60–75 pS (average 71 pS) in unsymmetrical K^+ solutions with outward current (Atwater et al., 1988). Most previous experiments have been performed in symmetrical high K^+ solutions, and various values ranging from ~100 to 300 pS have been reported for the unitary conductance (Barrett et al., 1982, Cook et al., 1984; Findlay et al., 1985; Atwater et al., 1988). The mean fraction open is very small (0–5%) at membrane potentials $\lesssim +25$ mV (Findlay, 1985). Some workers have therefore questioned the role of the K-Ca channel in bursting. Yet, according to the model (cf., Figs. 3 and 4 *a*), if the average total K-Ca conductance were much greater than 150–200 pS, the cell would be permanently hyperpolarized. Therefore only two to four K-Ca channels per cell can be open at any given time. Based on patch clamp experiments in which at least one K-Ca channel is found per 1 μm^2 patch (Andres Stutzin, personal communication), we estimate that there are several hundred K-Ca channels per cell. Thus, a small open fraction is actually a necessary condition for bursting in our model. The same observation also makes clear that a

single channel event can switch the cell between the spiking and silent regimes. We explore whether stochastic fluctuations of the K-Ca channel could produce the kind of irregular records observed in individual cells.

Of course, the other channels will also be undergoing stochastic fluctuations, but the K-Ca channel will have the most significant effect because it has the largest unitary conductance. A calculation of the standard deviations of the three currents shows that if the conductance of the K-Ca channel is, say, $10\times >$ that of the delayed-rectifier and $20\times >$ that of the calcium channel, then the fluctuations of the K-Ca current will dominate. Further support is found in the Chay-Kang (1988) model for cell clusters in which there is no K-Ca channel, and the largest channel is the delayed-rectifier. Fig. 3 in that study shows that the largest channel is responsible for the major part of the stochastic effects, and that the two smaller channels may safely be neglected.

We interpret the first order kinetic process represented by Eq. 2.3 as a Markov process in which the channel jumps from the open state to the closed state with probability per unit time $1/\tau_o$ and jumps back with probability per unit time $1/\tau_c$:

$$C \underset{1/\tau_o}{\overset{1/\tau_c}{\rightleftharpoons}} O \tag{3.1}$$

where τ_o and τ_c are then the mean open and closed times, respectively. Let N_o = the number of open channels and let N_c = the number of closed channels. The ratio of open to closed channels depends on τ_o and τ_c, and at equilibrium the ratio of their mean values is:

$$\frac{\langle N_o \rangle}{\langle N_c \rangle} = \frac{\tau_o}{\tau_c}. \tag{3.2}$$

In the deterministic model the fraction of open channels depends monotonically on intracellular calcium. This effect is achieved in the stochastic model by noting that τ_o depends on Ca_i (Cook et al., 1984; Findlay, 1985) and setting

$$\frac{\tau_o}{\tau_c} = \frac{Ca_i}{K_d}. \tag{3.3}$$

We generally keep τ_c fixed and let τ_o be proportional to Ca_i. If we let $p = N_o/(N_o + N_c)$ denote the fraction of open channels, then p is a random variable whose mean is the fraction of total K-Ca conductance in the deterministic case. For example, at equilibrium its mean value is

$$\langle p \rangle = \frac{\langle N_o \rangle}{\langle N_o \rangle + \langle N_c \rangle} = \frac{Ca_i}{K_d + Ca_i}. \tag{3.4}$$

Thus intracellular calcium provides a negative feedback mechanism, as in the deterministic case, but now it does so only indirectly by controling transition probabilities.

The associated system of stochastic equations is:

$$C_m \frac{dV}{dt} = -I_K - I_{Ca} - \bar{g}_{K\text{-}Ca} p(V - V_K) \tag{3.5}$$

$$\frac{dn}{dt} = \lambda \left[\frac{n_\infty(V) - n}{\tau_n(V)} \right] \tag{3.6}$$

$$\frac{dCa_i}{dt} = f(-\alpha I_{Ca} - k_{Ca} Ca_i), \tag{3.7}$$

where p is determined by the stochastic process described above. The three variable system of differential equations and stochastic process can be solved numerically as follows: given the values of V, n, Ca_i, and p at time t, use a numerical integrator to compute the values of V, n, and Ca_i at time $t + \Delta t$. Then use Ca_i to compute the probabilities of channel opening and closing and the fraction of channels open at $t + \Delta t$. We keep τ_c fixed and compute τ_o using the formula $\tau_o = \tau_c \cdot Ca_i/K_d$.

The probability that a given open channel will close during the interval $(t, t + \Delta t)$ is $\simeq$ to $\Delta t/\tau_o$, provided Δt is chosen sufficiently small. Since the channels are independent, the probability that one channel out of the population of open channels closes is $\Pr\{N_c \rightarrow N_c + 1, N_o \rightarrow N_o - 1\} = N_o \cdot \Delta t/\tau_o$.

We choose Δt so that this probability is <0.1, which assures that the probability of two openings is negligible. To decide if a channel closing occurs in our simulations, we use a random number generator to obtain a random variable, X, chosen from a uniform distribution on the interval $[0, 1]$. If $X < N_o \cdot \Delta t/\tau_o$, we increment N_c and decrement N_o by 1; otherwise we do nothing. We then proceed in the same manner to determine whether one of the closed channels opens during the interval $(t, t + \Delta t)$. The probability of this is $\Pr\{N_o \rightarrow N_o + 1, N_c \rightarrow N_c - 1\} = N_c \cdot \Delta t/\tau_c$.

Finally we compute p at $t + \Delta t$, $p = N_o/(N_o + N_c)$, and repeat the cycle.

For the benefit of readers who wish to perform these computations we make some additional comments on implementation. It is not necessary to monitor the state of each channel, but only the total number of channels in each state; this saves many calls to the random number generator. For a discussion of the validity of this simplification see (Keizer, 1987). When looked at in this way, the process is equivalent to a birth and death process (Cox and Miller, 1965). The time step must be chosen small enough to keep the error in the integration of the deterministic variables, V, n, and Ca_i small and also to keep the transition probabilities small, say <0.1 as suggested above. Our numerical integrator automatically chooses Δt so as to satisfy the first criterion; we use the option to specify a maximum allowable value for Δt to satisfy the second. Using the channel parameters discussed below, typical time steps were ~0.2 ms. Since bursts last many seconds (Fig. 1 *a*), hundreds of thousands of time steps are

required to do a complete simulation. Unlike the deterministic problem, which can easily be solved on a small personal computer with a numeric co-processor, the stochastic simulations require a fast mini-computer, such as a VAX 8600. The total CPU time is proportional to the number of time steps, hence the number of channels. In the next section we will discuss clusters of cells sharing thousands of channels, and for these simulations we found it convenient to use a CRAY X-MP super-computer (Cray Research, Inc., Mendota Heights, MN).

For the longest simulations presented below we used an alternative method to track the channel events that takes advantage of the fact that the time to the next event is exponentially distributed with rate parameter $N_o/\tau_o + N_c/\tau_c$. If the numbers of open and closed channels are at their equilibrium values, one can show that the average time between events is then

$$\frac{\tau_o + \tau_c}{2(N_o + N_c)} \tag{3.8}$$

with opening and closing probabilities

$$\Pr\{N_c \to N_c + 1, N_o \to N_o - 1\} = \frac{N_c/\tau_c}{N_o/\tau_o + N_c/\tau_c} \tag{3.9}$$

and

$$\Pr\{N_o \to N_o + 1, N_c \to N_c - 1\} = \frac{N_o/\tau_o}{N_o/\tau_o + N_c/\tau_c}. \tag{3.10}$$

(For a proof of the equivalence of this approach with the previous one see Cox and Miller, 1965). This time step is bigger than the one required by the previous method by a factor of ~5. We used this method in cases where the number of channels was very large, and the average time step was consequently very small. In this case a simpler Runge-Kutta integration scheme was found to be adequate for the deterministic variables. With this method, a simulation with 100,000 channels and an average time step of ~0.005 ms, can be carried out in <5 min of CRAY time. Like the previous method, the computation time is proportional to the number of channels and inversely proportional to the open and closed times, τ_o and τ_c.

In order to carry out a simulation we must choose values for the number of channels, N_{tot}, and for either τ_o or τ_c. Based on a density of ~1 K-Ca channel per 1 μm^2 patch we let $N_{tot} = 600$. For an assumed single-channel conductance $\hat{g}$ of 50 pS the total cell conductance $\bar{g}_{K\text{-}Ca}$ is 30,000 pS. From the Z-curve and the value of $\bar{g}_{K\text{-}Ca}$ we can predict that p will be ~0.005. We choose τ_c to be 1,000 ms and constant. From Eq. 3.3, τ_o will then vary with Ca_i and be ~5 ms. We have no data on τ_o for the K-Ca channel in the β-cell, but 5 ms. is compatible with data for rat muscle (Moczydlowski and Latorre, 1983). Finally, the calcium dissociation constant, K_d, is chosen to be 100 μM in order that Ca_i will be in the physiological range of ~0.5 μM. The value of Ca_i/K_d, and hence of K_d, is a constraint imposed by the Rorsman and Trube data and our estimate of $\bar{g}_{K\text{-}Ca}$; previously the Chay-Keizer model had used $K_d = 1$ μM.

Fig. 6 shows the results of a calculation with the above parameters, which should be compared with Fig. 1 *c*. The simulation for a single cell shows irregular spikes of large amplitude that range from the rest potential to nearly −10 mV. There is some evidence of abortive spiking from a plateau, as seen in the deterministic full islet model, but no evidence of bursting. Note that this simulation represents only a single sample path from the set of possible realizations of the stochastic process described above, rather than a unique solution to a set of equations as in the deterministic case. Other realizations can be obtained by varying the seed for the random number generator. The simulations reported here are typical ones taken from the many we have performed.

Fig. 7 *a* shows on an expanded time scale the portion of Fig. 6 with an overline. Spikes which begin at the rest potential, such as the first one in Fig. 7 *a*, are asymmetrical, with a slow upstroke and a rapid downstroke. Bangham et al. (1986) noted this in experimental records and attributed the rapid downstroke to sudden stochastic K-Ca channel openings. We believe that the downstroke is not much more rapid than in the deterministic case (compare Fig. 4 *b*), but rather that the upstroke is noticeably slower because the membrane time constant is relatively large at low voltages. Further analysis of the single-cell behavior is deferred to Section IV where it will be compared with results for clusters of cells.

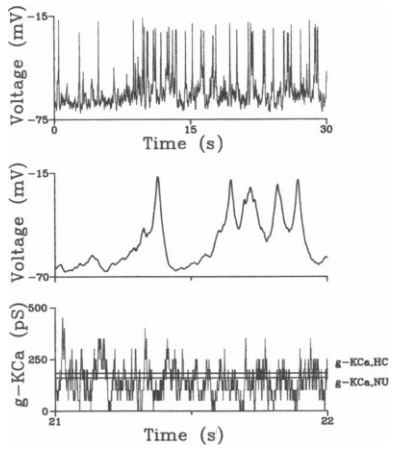

FIGURE 6 Simulated voltage time course for an isolated single cell with 600 50 pS K-Ca channels. Compare with Fig. 1 *c*. Voltage range of spikes is from the rest state to the maximum with no plateau, unlike a cell in an intact islet (Fig. 1 *a*) or the solution of the deterministic model (Fig. 5 *a*). The portion of the solution under the short horizontal line is expanded in Fig. 7 *a*.

FIGURE 7 Simulated single cell on expanded time scale. (*a*) Voltage and (*b*) $g_{K\text{-}Ca}$ time courses. Horizontal lines in Fig. 7 *b* indicate $g_{K\text{-}Ca,V}$, conductance level near which active phase begins and $g_{K\text{-}Ca,HC}$, conductance level near which active phase ends in deterministic model. This discreteness of the conductance levels is clearly visible. Note that $g_{K\text{-}Ca}$ can range far beyond the deterministic bounds.

In the absence of glucose, an isolated β-cell is quiescent (I. Atwater, personal communication). By reducing the calcium removal rate, k_{Ca}, to $\sim$0.0005 ms^{-1} we have obtained records of as long as 30 s without any spikes. This is remarkable considering the large variance of $\bar{g}_{K\text{-}Ca}$ when $k_{Ca} = 0.03$ ms^{-1} as in Fig. 6. In this case, the model predicts that Ca_i will approximately double to $\sim$1 μM. We plan to use the model in the future to contrast the glucose dose response of single cells and clusters of cells.

The stochastic model does a reasonable job of describing the behavior of an isolated β-cell. In the next section we show how to construct a cluster of stochastic β-cells that bursts.

IV. CLUSTERS OF TIGHTLY ELECTRICALLY-COUPLED CELLS

Channel Sharing Hypothesis

There is abundant experimental evidence that β-cells in an islet are electrically coupled, and morphological studies show the existence of gap junctions between β-cells (Eddlestone and Rojas, 1980; Meda et al., 1984). Lucifer Yellow dye injected into one cell through a microelectrode usually labels a small number (2–5) of neighboring cells (Michaels and Sheridan, 1981; Meda et al., 1986) presumably by passing through the gap junctions. Current injected in one cell produces an attenuated voltage response in neighboring cells, up to a separation of 40 μm (several cell diameters). Such direct local coupling, and perhaps other forms of coupling, contribute to long range effects throughout the islet, as indicated by the fact that the overall burst pattern is synchronized in cells up to 400 μm apart. This can be demonstrated by recording with two electrodes (Meda et al., 1984). Although individual spikes are not synchronized, even for larger separations there is only $\sim$1 s of phase lag in the burst pattern. One mechanism which may contribute to longer range coupling is the accumulation and diffusion of K^+ in the intercellular space.

Since the details of the coupling mechanism are as yet unknown, we make the assumption that β-cells in a cluster are sufficiently tightly coupled and that their membranes effectively share the entire pool of K-Ca channels. While this is an over-simplification, any amount of coupling will produce some channel sharing. As the size of the common pool increases the statistical variance of the K-Ca conductance, $g_{K\text{-}Ca}$, will decrease. We examine whether this reduction in statistical variance is sufficient to produce organized bursting.

Cluster Model (Stochastic)

We model a cluster as an ensemble of cells, identical in their gross properties and connected by zero resistance gap junctions. As a consequence of this idealization, the cluster is instantaneously isopotential and the ionic concentrations are identical in all the cells. It also follows that the surface-to-volume ratio of the cluster is independent of the number of cells, N_{cell}. Hence, C_m, I_K, and I_{Ca}, which are proportional to membrane surface area, scale with N_{cell}. Since $I_{K\text{-}Ca}$ depends on membrane area in the deterministic case and on the number of open channels in the stochastic case, it also scales with N_{cell}. One can think of such a cluster as either a single large cell or a collection of individual cells with perfectly synchronized electrical behavior.

With these simplifications, the deterministic and stochastic models for a single cell may be easily extended to a cluster. For the deterministic case, in fact, the cell and cluster equations are identical. For the stochastic case, the current balance equation needs a little care in its interpretation. Letting $\hat{g}$ be the single-channel conductance and N_o^i the number of open channels in the *ith* cell, Kirchoff's law for the cluster membrane is

$$N_{cell} C_m \frac{dV}{dt} = -N_{cell}(I_K + I_{Ca}) - \hat{g} \sum_{i=1}^{N_{cell}} N_o^i (V - V_K) \quad (4.1)$$

Dividing through by N_{cell} and multiplying and dividing the last term by $\bar{N}$, the number of channels per cell or channel density, Eq. 4.1 becomes

$$C_m \frac{dV}{dt} = -I_K - I_{Ca} - \hat{g}\bar{N} \frac{1}{N_{cell}\bar{N}} \sum_{i=1}^{N_{cell}} N_o^i (V - V_K) \quad (4.2)$$

or

$$C_m \frac{dV}{dt} = -I_K - I_{Ca} - \bar{g}_{K\text{-}Ca} p (V - V_K). \quad (4.3)$$

This equation is the same as for the single-stochastic cell (see Eq. 3.5) except that p must now be interpreted as the fraction of open channels in the cluster, while $\bar{g}_{K\text{-}Ca}$ is the total conductance per cell, as before. The remaining equations are unaltered. It follows from Eq. 4.2 that for a cluster the effective change in conductance due to a single-channel event is $\hat{g}/N_{cell}$, i.e., the event is shared equally by the membranes of all the cells in the cluster.

We remark that the simulation is completely determined by the values of $\bar{g}_{K\text{-}Ca}$, N_o, and N_c; the values of $\hat{g}$, $\bar{N}$, and N_{cell} can be deduced from $\bar{g}_{K\text{-}Ca}$, N_o, and N_c subject only to the consistency relations $\bar{g}_{K\text{-}Ca} = \hat{g} \cdot \bar{N}$ and $N_{tot} = N_o + N_c = \bar{N} \cdot N_{cell}$. Thus multiple interpretations can be given to a single simulation.

THEORETICAL RESULTS

Figs. 8 *a–d* show the results for a sequence of values of N_{cell}, obtained by increasing N_{tot} while keeping $\bar{g}_{K\text{-}Ca}$ fixed. Although simulations with 5 cells give voltage records not much different from a single cell, with 10 cells the spike amplitude is reduced and we begin to see some incipient bursts with spiking from a plateau. While these bursts are clearly defined, they are irregularly spaced and of variable duration. The 50-cell cluster shows fairly regular bursts with fluctuations in the length of the interburst interval and burst duration. The 167 cell cluster shows a further

increase in regularity. The amount of variability appears comparable with what is seen in experimental records from intact islets (Fig. 1 *a*) and large clusters (Fig. 1 *b*).

We now examine the process underlying the emergence of organized bursting demonstrated in the sequence comprising Figs. 6–8. As discussed in Section II, in the deterministic model $g_{K\text{-}Ca}$ follows Ca_i and in turn feeds back onto the membrane potential. The voltage-gated Ca^{2+} and K^+ currents determine a bursting window, marked as the interval ($g_{K\text{-}Ca,v}$, $g_{K\text{-}Ca,HC}$) in Figs. 4 *a* and 5 *d*, within which the total $g_{K\text{-}Ca}$ conductance must lie. Thus, the transition from the silent phase to the active phase occurs approximately when $g_{K\text{-}Ca}$ reaches $g_{K\text{-}Ca,v}$ and the transition from the active phase to the silent phase occurs when $g_{K\text{-}Ca}$ reaches $g_{K\text{-}Ca,HC}$.

From Figs. 7, *a* and *b* we can see that it is not appropriate to apply the bifurcation analysis of the deterministic model in this case because $g_{K\text{-}Ca}$ changes rapidly on the time scale of a single spike, violating the quasi-steady state assumption. Indeed, single-channel events can cause the conductance to jump over the entire deterministic burst window (indicated by the two horizontal lines in Fig. 7 *b*). Ca_i (not shown) is essentially constant during this time; the spiking is entirely due to the interaction between the stochastic fluctations and the *V-n* spike generating mechanism. Nonetheless, when the average $g_{K\text{-}Ca}$ stays above $g_{K\text{-}Ca,HC}$ for a sufficiently long time the cell becomes hyperpolarized, and when $g_{K\text{-}Ca}$ stays below $g_{K\text{-}Ca,v}$ spiking can occur. Because the fluctuations in $g_{K\text{-}Ca}$ are so rapid, most bursts consist of only one or two spikes. The burst with four spikes shown in Fig. 7 *b* is a relatively rare occurrence.

In the single-cell case the changes in the mean value of $g_{K\text{-}Ca}$, which is determined by Ca_i, are overwhelmed by statistical fluctations. Thus, Ca_i varies in response to the changes in membrane potential through the voltage-dependent calcium current but has little influence on $g_{K\text{-}Ca}$. As the number of cells increases, the variance of $g_{K\text{-}Ca}$ decreases and the regulatory role of Ca_i is enhanced. In Figs. 9 *a–c* we have plotted the voltage, $g_{K\text{-}Ca}$, and calcium time courses for the case of a 50 cell cluster, the first case shown which exhibits organized bursting (Fig. 9 *a* is the same as Fig. 8 *c*, repeated for clarity). Although the variance of $g_{K\text{-}Ca}$ is still large, its time course now visibly follows the mean determined by Ca_i and stays close to the bursting window, except for rare large excursions. It is perhaps not surprising that the behavior of the stochastic model converges to that of the deterministic model as the number of cells increases, but it is remarkable that bursts are seen even while the stochastic fluctuations are still quite large.

Another observation is that the variance of the minimal values of Ca_i is much smaller than that of the maximal values, and that the minimal values are much closer to Ca_v than the maximal values are to Ca_{HC}. We attribute this asymmetry to the difference in membrane time constants

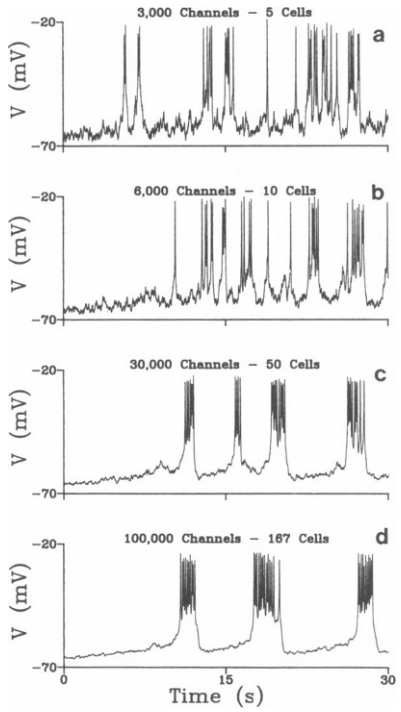

FIGURE 8 Voltage time courses for different sized clusters: 5, 10, 50, and 167 cells respectively in *a–d;* each cell has 600 50 pS channels, as in Figs. 6 and 7. There is a transition from irregular spiking to organized bursting as the number of channels and hence the number of cells increases. Burst period increases with the number of channels and approaches that of the deterministic model from below. Compare *c* and *d* with Figs. 1, *a* and *b*.

between the high-voltage active phase and the low-voltage silent phase. During the active phase the time constant is much smaller and the membrane potential is therefore much more sensitive to brief perturbations. During the silent phase the membrane response is slower, and more sustained variations in the average conductance (which are crudely reflected in the value of Ca_i) are required to depolarize the membrane enough to initiate spiking.

Another view of this behaivor is shown in the *V*-Ca_i phase plane (Fig. 9 *d*). (Unlike the deterministic case, in which the *V*-Ca_i and *V*-$g_{K\text{-}Ca}$ phase planes are essentially interchangeable, the *V*-$g_{K\text{-}Ca}$ phase plane is so noisy that it does not convey much information.) We can see that not only is there variation in the points where the trajectory exits from the active phase, but that there is a systematic bias towards premature termination of the active phase. Random fluctuations in $g_{K\text{-}Ca}$ can drive the voltage below threshold. As the number of cells is made still larger the points of exit from the active phase approach the homoclinic point, Ca_{HC}. That is, organized bursting allows longer active phases and higher levels of intracellular calcium. This observation suggests that bursting plays a role in enhancing secretion. Chay and Kang (1988) make the same point.

The above simulations demonstrate that moderately sized clusters of cells can exhibit organized bursting and

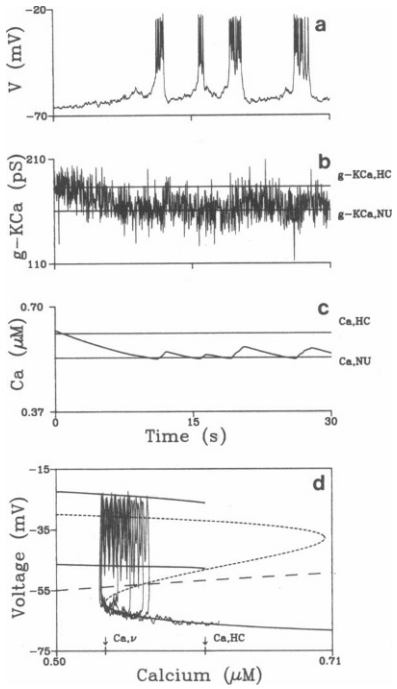

FIGURE 9 (*a*) Voltage time course for 50-cell cluster (same as Fig. 8 *c*). (*b*) $g_{K\text{-}Ca}$ and (*c*) Ca_i plotted against time. Although variance is still large, $g_{K\text{-}Ca}$ follows the mean determined by Ca_i much more closely than the 1, 5, or 10 cell cases. Active phases are correlated with, but not exactly determined by time periods when $g_{K\text{-}Ca}$ is below $g_{K\text{-}Ca,\nu}$, and silent phases are correlated with periods when $g_{K\text{-}Ca}$ is above $g_{K\text{-}Ca,HC}$. Brief, large excursions cause only small perturbations. The variance of the maxima of Ca_i is much greater than that of the minima because of the smaller membrane time constant during the active phase. The knee and the homoclinic point are expressed in terms of calcium: Ca_ν = 0.5372 and Ca_{HC} = 0.6146. (*d*) *V*-Ca trajectory superimposed on bifurcation diagram. Compare with Fig. 5 *d*. There is a systematic bias towards premature termination of the burst and hence short burst period because of stochastic fluctuations in $g_{K\text{-}Ca}$.

support the idea that the difference in behavior between single β-cells and clusters is due at least in part to channel sharing. Some caution, however, is necessary in drawing quantitative conclusions. The set of parameters used to generate Figs. 6–8, while perfectly defensible, was chosen to achieve a relatively large bursting window, Δg. With some other, not unreasonable, parameter sets that result in a much smaller Δg, a much larger number of cells is required to achieve regular bursting. The results also depend on the values chosen for $\hat{g}$ and $\bar{N}$. We cannot completely account for the dependence of the number of cells required for bursting on the model parameters, but we give some partial results below.

Recall from Eq. 4.4 that the conductance perturbation due to a single-channel event is $\hat{g}/N_{cell}$. For organized bursting, this quantity should be small compared with Δg, and this is guaranteed as the number of cells increases. The width of the burst window, as measured in channel events, is $\Delta g N_{cell}/\hat{g}$. Intuitively, one expects that as this quantity increases the average duration of the silent and active phases will increase, asymptotically approaching the values seen in Fig. 5 as $N_{cell} \to \infty$, and this is in fact what is seen. One also expects the emergence of regular bursting to be facilitated by small $\hat{g}$. Support for this prediction is obtained below. Larger Δg should also promote the emergence of bursting. This effect is much harder to study systematically, but we have confirmed its importance for selected cases.

TABLE I
EFFECT OF VARYING $\hat{g}$ AND $\bar{N}$ WHILE KEEPING $\bar{g}_{K\text{-}Ca}$ FIXED

$\hat{g}$	$\bar{N}$	$\bar{g}_{K\text{-}Ca}$	p	N_{cell}
50	600	30,000	0.005	$N_{tot}/600$
10	3,000	30,000	0.005	$N_{tot}/3{,}000$

A given simulation may be interpreted as corresponding to different unitary conductances, channel densities, and numbers of cells provided the total K-Ca conductance is held fixed. For example, suppose the single-channel conductance, $\hat{g}$, is increased by a factor of five and the number of channels per cell, $\bar{N}$, is reduced by the same factor, leaving $\bar{g}_{K\text{-}Ca}$ unchanged. The Monte Carlo channel simulation will be unchanged (provided it is started with the same random number generator seed) but the number of cells will increase by a factor of five. This is spelled out in Table I.

More formally, we can say that the simulations described in Section IV are invariant, for an arbitrary scale factor γ, under the transformation $\hat{g} \to \hat{g}/\gamma$, $\bar{N} \to \gamma \bar{N}$, but the interpretations are different: for a given total conductance, $\bar{g}_{K\text{-}Ca}$, fewer cells are required for bursting if the single-channel conductance is smaller. This conclusion satisfies our intuition that a fine grain is more deterministic than a coarse grain.

Suppose now that the value we use for $\bar{g}_{K\text{-}Ca}$ is incorrect because our estimate of $\hat{g}$ or of $\bar{N}$ is too small by a factor γ. What effect would this have on our conclusions? For example, suppose that $\bar{g}_{K\text{-}Ca}$ is doubled because we revise our estimate for $\hat{g}$ while keeping channel density fixed. The average fraction of channels open, p, will be automatically halved to keep the average total K-Ca conductance in the bursting regime. A calculation using Eqs. 3.3, 3.4, and 3.8–10 shows that if p is small and the total number of channels, N_{tot}, and the mean closed time, τ_c, are increased by a factor of two, the simulation will be virtually unchanged. It follows that in order to maintain equally regular bursting it is sufficient to double N_{tot} and τ_c. The

TABLE II
EFFECT OF VARYING $\bar{g}_{K\text{-}Ca}$

$\bar{g}_{K\text{-}Ca}$	$\hat{g}$	$\bar{N}$	p	τ_c	τ_0	N_{cell}
30,000	50	600	0.005	1s	5 ms	$N_{tot}/600$
60,000	100	600	0.0025	2s	5 ms	$2N_{tot}/600$
60,000	50	1,200	0.0025	2s	5 ms	$2N_{tot}/1{,}200$

upshot is that the number of cells required to achieve a given degree of regularity of bursting would be doubled if $\bar{g}_{K\text{-}Ca}$ were doubled. This case corresponds to the first two lines in Table II.

If, on the other hand the increase in $\bar{g}_{K\text{-}Ca}$ were due to an increase in channel density alone, the number of channels would increase, but the number of cells would not be changed; see line three of Table II. Table II can be summarized formally as follows: if p is small, the Monte Carlo simulation is invariant, to first order in p, under the transformation $\bar{g}_{K\text{-}Ca} \rightarrow \gamma \cdot \bar{g}_{K\text{-}Ca}, p \rightarrow p/\gamma, N_{tot} \rightarrow \gamma \cdot N_{tot}$, $\tau_c \rightarrow \gamma \cdot \tau_c$, and this multiplies the value of N_{cell} required to achieve a given degree of burst reularity by γ. While this adjustment in N_{tot} and τ_c is sufficient to restore burst regularity, it is not necessary. Empirically, if τ_c is kept fixed, regularity can be maintained by a somewhat larger increase in N_{tot}.

We would like to be able to predict quantitatively the effects of changing N_{tot} alone, as in Fig. 8, and of other transformations not covered by the invariances above. Further numerical work and analysis of the underlying stochastic process, which can be interpreted as an Ornstein-Uhlenbeck process with drift (Cox and Miller, 1965), are necessary to elucidate these relationships.

In summary, our theoretical results show that tightly electrically coupled cells with stochastic conductances modulated by slow variables can generate increasingly regular bursts as the number of cells increases. We have obtained some results about how the number of cells needed to obtain a given level of regularity depends on the simulation parameters. For example, (*a*) for fixed $\bar{g}_{K\text{-}Ca}$, the number of cells required is proportional to $\hat{g}$ (Table I). (*b*) For fixed $\bar{N}$, the number of cells required is proportional to $\bar{g}_{K\text{-}Ca}$, provided τ_c is adjusted in the same proportion. (Table II, lines 1 and 2). (*c*) For fixed $\hat{g}$, the number of cells is independent of $\bar{g}_{K\text{-}Ca}$, provided τ_c is adjusted (Table II, lines 1 and 3). Finally, (*d*) the number of cells varies inversely, in an as yet undetermined way, with the size of the bursting window, Δg, provided τ_c is adjusted. These theoretical conclusions depend only on the qualitative geometrical structure of the phase plane and the separation into fast and slow variables. Otherwise they are independent of the precise mechanism of bursting. In the next section we discuss their application to the β-cell.

V. DISCUSSION

We have modified the Chay-Keizer model for the β-cell as studied in the intact islet preparation. The model is in reasonable agreement with known experimental measurements and is simple enough to be easily modified as new data become available. It is also robust enough under parameter changes to reflect the natural variability of β-cells. It cannot account, however, for the irregular electrical behavior of isolated β-cells.

We have demonstrated a stochastic extension of the model which can capture the behavior of single cells (Compare Figs. 6 and 7 with Fig. 1 *c*), large clusters of cells (Compare Fig. 8 *c* with Fig. 1 *b*), and whole islets (Compare Fig. 8 *d* with Fig. 1 *a*), depending solely on the mechanism of channel sharing. We feel that this study has established the viability of the channel sharing hypothesis as at least part of the explanation of this phenomenon. Some of our conclusions depend on the values of parameters which are not precisely known. We have tried to indicate some of these dependencies in section IV, although more work needs to be done. As further experiments are carried out and parameter values are revised, it may turn out that enormous numbers of cells would be required theoretically to obtain reasonable bursts. In that case we would have to re-evaluate the hypothesis that bursting is the result of sharing K-Ca channels.

Our simulations also indicate a possible role for bursting in enhancing the β-cell's primary function of secretion. As the number of cells coupled in a cluster increases and bursting becomes more regular, intracellular calcium levels increase. See Figs. 9 *c* and 5 *c* for the 50 cell and deterministic cases, and see Chay and Kang (1988) Fig. 4 for a systematic study. Increased coupling caused by prolactin has been correlated with increased insulin secretion in vivo (Michaels, et al., 1987).

We have neglected the effect of another class of K^+ channels, the ATP-blockable (K-ATP) channel (Cook and Hales, 1984; Ashcroft et al., 1984; Ashcroft et al., 1987). Magnus (1988) and Keizer (1987*b*) have investigated the possibility that the K-ATP current regulates bursting by calcium feedback on ADP/ATP ratios. In their model the K-ATP conductance is a monotonically increasing, saturated function of instantaneous intracellular calcium similar to the K-Ca conductance in our model, and bursting can be obtained by replacing the K-Ca current with a K-ATP current. Like the K-Ca channel, the role of the K-ATP channel in bursting has been questioned because it is rarely open in the presence of glucose. Nonetheless, there are so many K-ATP channels present that they may carry substantial total current. One could develop a stochastic model for the K-ATP channel along the same lines as for the K-Ca channel. Our theoretical results (see Tables I and II) suggest that the smaller conductance of the ATP-blockable channel would allow regular bursting with smaller clusters than with the K-Ca channel. This phenomenon is also seen in the model of Chay and Kang (1988), where the major stochastic effect is from the delayed-rectifier channel. Since it is much smaller than the K-Ca channel, bursting is achieved with many fewer cells than in our model. Incidentally, that model also shows that it is not necessary for the stochastic fluctuations which disrupt bursting to result from the channel which regulates the burst.

It is most likely that both the K-Ca and K-ATP channels play a role in bursting. It is easy to accommodate mixed populations of stochastic channels in our model. If one distributes a given amount of total maximal conductance

between two populations of channels, it can be shown that the variance of the total slow potassium conductance will be intermediate between those of the pure populations. The same analysis shows that even if most of the potassium current is carried by the smaller K-ATP channels, the variance of the larger K-Ca channels may still be considerable. Simulations, along the lines described in the previous section, with a single stochastic K-Ca channel and a deterministic slow potassium conductance show that bursts can be disrupted if the stochastic channel opens near threshold during spiking. The impact of this effect depends on the rate of openings per unit time of the stochastic channel and the size of the mean open time of the channel relative to the membrane time constant. The conclusion we draw from this simulation is that any model for the β-cell bursting mechanism must be able to tolerate the perturbations caused by the K-Ca channels.

We realize that our model for coupling is very idealized. We ignore the gap junctional resistance which would cause time delays in, and attenuation of, the influence of cells on their neighbors. We also ignore heterogeneity in the properties of cells as oscillators. These neglected factors would tend to weaken the coupling, reduce the degree of synchronization of the β-cells in the islet, and render it more difficult for moderate-sized clusters of cells to exhibit regular bursting. Nevertheless, we feel that the model presented here sheds light on the behavior of small clusters of tightly-coupled cells, such as are revealed by dye coupling experiments. Further, we feel that one way to understand the emergence of organized bursting in large cell clusters and islets is through the coupling of these small clusters by accumulation and diffusion of K^+ in intercellular spaces. We hope to assess the role of such factors with more detailed models which may include resistive gap junctions, ionic diffusion, and perhaps individual variability in one or more key parameters.

We have made other simplifications which are probably not important for the conclusions. Our model for the handling of the calcium that comes into the cell is crude. There has been much speculation and theoretical modeling about small domains with high local concentrations of Ca^{2+} near the cell membrane (Chad and Eckert, 1984; Simon and Llinas, 1985). This has been offered as an alternative explanation for the fact that the K-Ca channels are open so infrequently at the typical free intracellular calcium concentrations (Velasco and Petersen, 1987). We have ignored this issue partly for simplicity, and partly because we wanted to investigate whether infrequently open channels could play a role in the cell without invoking other hypotheses.

Some known features have been left out of the model. There is a small amount of inactivation, perhaps Ca^{2+} dependent, of the Ca^{2+} channel (Plant, 1987). As mentioned in Section II, the appropriate way to model the calcium current needs further study. There is also some voltage-dependent inactivation of the delayed-rectifier channel, which we have found to be unimportant. We have ignored the voltage dependence (Cook et al., 1984; Findlay et al., 1985; Velasco and Petersen, 1987) and time constant of the K-Ca channel because we feel that the existing data in the low voltage and low calcium regime do not justify quantitative modeling at this time.

We hope that this study will be provocative to experimentalists. The viability of channel sharing is critically dependent on the size of the bursting window, Δg, which in turn depends sensitively on the reversal potentials V_K and V_{Ca}, and the dynamic parameters for the voltage-gated potassium and calcium channels, V_n and λ. We know of no measurements of the range of K-Ca conductance experienced during a burst; our deterministic spike dynamics constrain it to lie in the interval (150 pS, 200 pS) if $\bar{g}_K$ = 2,500 pS and $\bar{g}_{Ca}$ = 1,400 pS. Our results also depend on the values of $\bar{g}_{K\text{-}Ca}$, τ_o, τ_c, $\bar{N}$, $\hat{g}$, and p. The product $p\bar{g}_{K\text{-}Ca}$ must lie within the bursting interval; with $\bar{g}_{K\text{-}Ca}$ = 30,000 pS p must be ~0.005. This figure is not incompatible with experimental values obtained so far (Findlay, 1985; Velasco and Petersen, 1987). We made reasonable guesses for the values of the mean open and closed times, τ_o and τ_c, and for the channel density since values for these quantities have not been reported. Our value for τ_o of ~5 ms is compatible with data from rat muscle (Moczydlowski and Latorre, 1983).

It would be helpful to have reliable values fo the β-cell, although we found that, with the parameters used here, the numerical results showed little qualitative change as τ_c was varied from 250 ms to 30 s. (We have found other cases in which the value of τ_c does make a significant difference.) There is a large discrepancy in the measured unitary conductance of the K-Ca channel depending on whether symmetrical and unsymmetrical K^+ solutions are used (Atwater et al., 1988), and it would be useful if the physiologically relevant value were determined. Of course, the values for all these parameters are constrained to be consistent with each other; for example, it is necessary that $g_{K\text{-}Ca} = p\bar{g}_{K\text{-}Ca}$, $p = \tau_o/(\tau_o + \tau_c)$ and $\bar{g}_{K\text{-}Ca} = \hat{g}\bar{N}$.

In addition to obtaining this valuable information on the channel level, it would be most helpful to have additional experimental confirmation of the predictions of the model by systematically recording from clusters of reaggregated cells. If the model is correct, one should be able to observe abortive bursts and drift in burst period over long runs. Perhaps it is even possible to measure the regularity of bursting as a function of cluster size. Cells from mice injected with glyburide show increased gap junctions as measured by dye coupling (Meda et al., 1979; Meda et al., 1984). Thus, one might create artificial clusters with a high degree of coupling and varying numbers of cells, like the theoretical ones here. The variance of burst and silent phase duration could then be measured and compared with numerical results from the model. The extent of coupling can also be dramatically increased by prolactin (Michaels et al., 1987). Similar experiments (Clay and DeHaan,

1979) have been performed on chick heart ventricular cells which are tightly coupled and exhibit rhythmic pacemaker activity. The variance of the interbeat interval was shown experimentally to decrease as $N^{-1/2}$, where N is the number of cells in the cluster. This result has been supported theoretically by simulations of stochastic sodium and potassium channels in patches of squid axon of varying area (Clay and DeFelice, 1983). Even qualitative data of this type for the β-cell could be of great help in understanding synchrony and evaluating the channel-sharing hypothesis.

APPENDIX

Equations and Parameters

Equations for the Deterministic Model:

$$C_m(dV/dt) = -\bar{g}_K n\,(V - V_K) - \bar{g}_{Ca} m_\infty(V) h(V)\,(V - V_{Ca}) - g_{K\text{-}Ca}(Ca_i)(V - V_K),$$

$$dn/dt = \lambda\,[n_\infty(V) - n/\tau_n(V)],$$

$$dCa_i/dt = f(-\alpha I_{Ca} - k_{Ca}\,Ca_i),$$

where

$$g_{K\text{-}Ca}\,(Ca_i) = \bar{g}_{K\text{-}Ca}\,(Ca_i/K_d + Ca_i),$$

$$m_\infty(V) = 1/1 + \exp\,([V_m - V]/S_m),$$

$$h(V) = 1/1 + \exp\,([V - V_h]/S_h),$$

$$n_\infty(v) = 1/1 + \exp\,([V_n - V]/S_n), \tau_n(V) = c/\exp\,([V - \bar{V}]/a) + \exp\,(-[V - \bar{V}]/b),$$

and

$$\alpha = 1/2\,V_{cell}F.$$

Standard Parameter Values[2]

Parameter	Definition/first use	Numerical value
units		
r (μm)	Cell radius	6.5
C_m (fF)	Total capacitance	5,310
V_{cell} (μm^3)	Cell volume	1,150
F (Coul/mMol)	Faraday constant	96.487
V_m (mV)	Eq. 2.1	4
S_m (mV)	Eq. 2.1	14
V_n (mV)	Eq. 2.2	−15
S_n (mV)	Eq. 2.2	5.6
a (mV)	Eq. 2.3	65
b (mV)	Eq. 2.3	20
c (ms)	Eq. 2.3	60
$\bar{V}$ (mV)	Eq. 2.3	−75
V_h (mV)	Eq. 2.4	−10
S_h (mV)	Eq. 2.4	10
$\bar{g}_K$ (pS)	Eq. 2.5	2,500
$\bar{g}_{Ca}$ (pS)	Eq. 2.5	1,400
V_K (mV)	Eq. 2.5	−75
V_{Ca} (mV)	Eq. 2.5	+110
λ	Eq. 2.7	1.7
K_d (μM)	Eq. 2.8a	100
$\bar{g}_{K\text{-}Ca}$ (pS)	Eq. 2.9	30,000
f	Eq. 2.10	0.001
k_{Ca} (ms^{-1})	Eq. 2.10	0.03

[2]These values used except where noted in text.

The authors would like to thank Dr. Jacob Maizel, Chief of the Laboratory of Mathematical Biology, National Cancer Institute, and the staff of the Advanced Scientific Computing Laboratory, in Frederick, Maryland for providing the computer time and technical support necessary for the successful completion of this project.

J. E. Keizer gratefully acknowledges supports from the National Science Foundation grant CHE 86-18647, the John Simon Guggenheim Memorial Foundation, a sabbatical leave form the University of California, Davis, and the hospitality of the Mathematical Research Branch at the National Institutes of Helath.

The work of A. S. Sherman was supported by a National Research Council-National Institutes of Health Research Associateship.

Received for publication 25 January 1988 and in final form 11 April 1988.

REFERENCES

Ashcroft, F. M., D. E. Harrison, and S. J. H. Aschroft. 1984. Glucose induces closure of single potassium channels in isolated rat pancreatic B-cells. *Nature (Lond.)*. 312:446–448.

Ashcroft, F. M. 1987. Adenosine 5'-triphosphate-sensitive potassium channels. *Annu. Rev. Neurosci.* 11:97–118.

Atwater, I., C. M. Dawson, A. Scott, G. Eddlestone, and E. Rojas. 1980. The nature of the oscillatory behavior in electrical activity for pancreatic β-cell. *J. of Horm. Metabol. Res.* 10 (suppl.):100–107.

Atwater, I., L. Rosario, and E. Rojas. 1983. Properties of calcium-activated potassium channels in the pancreatic β-cell. *Cell Calcium.* 4:451–461.

Atwater, I., and J. Rinzel. 1986. the β-cell bursting pattern and intracellular calcium. *In* Ionic Channels in Cells and Model Systems. R. Latorre, editor. Plenum Publishing Co., New York and London. 353–362.

Atwater, I., M. X. Li, E. Rojas, and A. Stutzin. 1988. Glucose reduces both ATP-blockable and Ca-activated K-channel activity in cell-attached patches from rat pancreatic B-cells in culture. *Biophys. J.* 53:145*a*. (Abstr.)

Bangham, J. A., P. A. Smith, and P. C. Croghan. 1986. Modeling the beta-cell electrical activity. *In* Biophysics of the Pancreatic β-Cell. I. Atwater, E. Rojas, and B. Soria, editors. Plenum Publishing Co., New York and London. 265–278.

Barrett, J. N., K. L. Magleby, and B. S. Pallotta. 1982. Properties of single calcium-activated potassium channels in cultured rat muscle. *J. Physiol. (Lond.)*. 331:211–230.

Beigelman, P. M., B. Ribalet, and I. Atwater, 1977. Electrical activity of mouse pancreatic beta-cells. II. Effects of glucose and arginine. *J. Physiol. (Paris). 73:201–217.*

Chad, J. E., and R. Eckert. 1984. Calcium domains associated with individual channels can account for anomalous voltage relations of Ca-dependent responses. *Biophys. J.* 45:993–999.

Chay, T. R., and J. Keizer. 1983. Minimal model for membrane oscillations in the pancreatic β-cell. *Biophys. J.* 42:181–190.

Chay, T. R., and J. Keizer. 1985. Theory of the effect of extracellular potassium on oscillations in the pancreatic β-cell. *Biophys. J.* 48:815–827.

Chay, T. R., and H. S. Kang. 1988. Role of Single-Channel Stochastic Noise on Bursting Clusters of Pancreatic β-Cells. *Biophys. J.* 54:427–435.

Clay, J. R., and R. L. DeHaan. 1979. Fluctuations in interbeat interval in rhythmic heart-cell clusters. *Biophys. J.* 28:377–390.

Clay, J. R., and L. J. DeFelice. 1983. Relationship between membrane excitability and single-channel open-close kinetics. *Biophys. J.* 42:151–157.

Cook, D. L., and C. N. Hales. 1984. Intracellular ATP directly blocks K^+ channels in pancreatic B-cells. *Nature (Lond.)*. 311:271–273.

Cook, D. L., M. Ikeuchi, and W. Y. Fujimoto. 1984. Lowering of pH inhibits calcium-activated potassium channels in isolated rat pancreatic islet cells. *Nature (Lond.)*. 311:269–271.

Cox, D. R., and H. D. Miller. 1965. The Theory of Stochastic Processes. John Wiley and Sons, Inc., New York.

Dean, P. M., and E. K. Mathews. 1970. Glucose-induced electrical activity in pancreatic islet cells *J. Physiol. (Lond.)*. 210:255–264.

Doedel, E. 1981. AUTO: A program for the automatic bifurcation analysis of autonomous systems. *Cong. Num.* 30:265–284.

Eddlestone, G. T., and E. Rojas. 1980. Evidence of electrical coupling between mouse pancreatic β-cells. *J. Physiol. (Lond.)*. 303:76–77P.

Findlay, I., M. J. Dunne, and O. H. Peterson. 1985. High-conductance K^+ channel in pancreatic islet cells can be activated and inactivated by internal calcium. *J. Membr. Biol.* 83:169–175.

Fitzhugh, R. 1961. Impulses and physiological states in theoretical models of nerve membrane. *Biophys. J.* 1:445–466.

Gear, C. W. 1967. The numerical integration of ordinary differential equations. *Math. Comp.* 21:146–156.

Goldman, D. E. 1943. Potential, impedance, and rectifications in membranes. *J. Gen. Physiol. (Lond.)*. 27:36–60.

Hodgkin, A. L., and B. Katz. 1949. The effect of sodium ions on the electrical activity of the giant axon of the squid. *J. Physiol. (Lond.)*. 108:37–77.

Kay, A. R., and R. K. S. Wong. 1987. Calcium current activation kinetics in isolated pyramidal neurones of the CA1 region of the mature guinea-pig hippocampus, *J. Physiol. (Lond.)*. 392:603–616.

Keizer, J. E. 1987. Statistical Thermodynamics of Nonequilibrium Processes. Springer-Verlag, New York. 135–138.

Keizer, J. E. 1988. Electrical activity and insulin release in pancreatic beta cells. *Math. Biosci.* In press.

Magnus, J. 1988. PhD Thesis. University of California, Davis. In press.

Meda, P., A. Perrelet, and A. Orci. 1979. Increase of gap junctions between pancreatic β-cells during stimulation of insulin secretion. *J. Cell Biol.* 82:441–448.

Meda, P., I. Atwater, A. Gonçalves, A. Bangham, L. Orci, and E. Rojas. 1984. The topography of electrical synchrony among β-cells in the mouse Islet of Langerhans. *Q. J. Exp. Physiol.* 69:719–735.

Meda, P., R. M. Santos, and I. Atwater. 1986. Direct identification of electrophysiologically monitored cells within intact mouse Islets of Langerhans. *Diabetes.* 35:232–236.

Michaels, R. L., and J. D. Sheridan. 1981. Islets of Langerhans: dye coupling among immunocytochemically distinct cell types. *Science (Wash., DC)*. 214:801–803.

Michaels, R. L., R. L. Sorenson, J. A. Parsons, and J. D. Sheridan. 1987. Prolactin enhances cell-to-cell communication among β-cells in pancreatic islets. *Diabetes.* 36:1098–1102.

Moczydlowski, E., and R. Latorre. 1983. Gating kinetics of Ca^{2+}-activated K^+ channels from rat muscle incorporated into planar lipid bilayers. *J. Gen. Physiol.* 82:511–542.

Morris, C., and H. Lecar. 1981. Voltage oscillations in the barnacle giant muscle fiber. *Biophys. J.* 35:193–213.

Plant, R. E. 1978. The effects of calcium++ on bursting neurons. A modeling study. *Biophys. J.* 21:217–237.

Plant, T. D. 1987. Calcium current inactivation in cultured mouse pancreatic islet cells is calcium-dependent. *J. Physiol. (Lond.)*. 390:86P.

Rinzel, J. 1985. Bursting oscillations in an excitable membrane model. *In* Ordinary and Partial Differential Equations. B. D. Sleeman and R. J. Jarvis, editors. Springer-Verlag, New York. 304–316.

Rorsman, P., and G. Trube. 1986. Calcium and delayed potassium currents in mouse pancreatic β-cells under voltage clamp conditions. *J. Physiol. (Lond.)*. 375:531–550.

Rubin, R. P. 1982. Calcium and Cellular Secretion. Plenum Publishing Co., New York and London.

Simon, S. M., and R. R. Llinas. 1985. Compartmentalization of the submembrane calcium activity during calcium influx and its significance in transmitter release. *Biophys. J.* 48:485–498.

Velasco, J. M., and O. H. Petersen. 1987. Voltage-activation of high-conductance K^+ channel in the insulin-secreting cell line RINm5F is dependent on local extracellular Ca^{2+} concentration. *Biochim. Biophys. Acta.* 896:305–310.